International Journal of Fracture 34: 3–22 (1987)

Fracture of nonhomogeneous materials

J.W. EISCHEN
Department of Mechanical and Aerospace Engineering, Campus Box 7910, North Carolina State University, Raleigh, NC 27695, USA

Received 20 June 1986; accepted in revised form 11 December 1986

Abstract. The nonhomogeneous materials considered in this work are of a class whose elastic moduli are specified by continuous and generally differentiable functions of the spatial coordinates. The elastic stress and displacement fields near a crack tip in a two-dimensional nonhomogeneous cracked body are derived utilizing an extension of the Williams eigenfunction expansion technique. The nature of the stress and strain singularity is ascertained to be precisely of the same form as the well-known inverse square root stress singularity near a crack tip in a homogeneous material, independent of the functional form of the elastic moduli variation. A new quasi-path-independent integral has been generated which proves useful for computing the energy release rate and mixed-mode stress intensity factors in nonhomogeneous cracked bodies. The integral is used in conjunction with finite element analysis for purposes of computing stress intensity factors. Numerical results are compared with certain exact solutions which are available for nonhomogeneous cracked bodies. Cracked composite bodies have traditionally been modeled and analyzed as possessing discontinuous elastic moduli, but are treated here as having rapid, but smooth variations of the material properties.

1. Introduction and background

Current engineering designs frequently involve situations where nonhomogeneous materials are either present naturally, or are used intentionally to attain a required structural performance. The elastic moduli depend on position in a nonhomogeneous material. Generally, two classes of such nonhomogeneous materials are discussed. The first class features an abrupt discontinuity in the magnitude of the material constants, such as in laminated composite structures. The second class involves materials where the elastic moduli vary smoothly. Soils, foundations, and geologic structures are all examples of where such a variation occurs naturally. When intentional bonding of two materials creates a smooth, but rapid variation in the elastic moduli near an interface, another example of the second class occurs. Issues relevant to fracture analysis of this latter class of materials form the main impetus of this paper.

Many researchers have been concerned with developing solutions for the states of stress and strain near crack tips located in composite media. For analytical purposes, composites are normally idealized as structures possessing elastic moduli which are only piecewise constant. In reality, abrupt discontinuities in the elastic moduli cannot exist because the interface between solids of differing elastic constants must be diffuse. For example, when two such solids are bonded, the material in the proximity of the bond possesses continuous, rapidly varying elastic moduli. The elastic fields around a crack tip which resides in a material whose elastic moduli are continuous functions of position must be understood in order to predict the fracture susceptibility of such materials. The elastic crack tip fields in such materials have not been studied nearly as vigorously as problems which have been

modeled, at least mathematically, as containing abrupt modulus changes. Interest in media with smoothly varying moduli have arisen partly because of possible applications to soil mechanics and geophysics. It is known that the rigidity of natural soils increases with distance from the surface of the earth (see Kassir [1]), and therefore the analysis of crack-like features necessitates an understanding of the fracture of nonhomogeneous materials. Fuse-bonded materials used in the electronics industry also exhibit characteristics of the type being discussed.

The work reported in this paper has been directed towards finite element computation of fracture parameters (stress intensity factors) in cracked bodies of arbitrary geometrical configuration whose elastic moduli are "smooth" functions of the spatial coordinates. Successful numerical work pertaining to fracture mechanics hinges on a fundamental understanding of the elastic crack tip fields. As a precursor to the numerical work, several theoretical issues were settled. In a recent paper by Delale [2], the following statement was made: "Even though no systematic study of the problem appears to have been made, it is reasonable to expect that in nonhomogeneous materials with continuous and generally differentiable elastic moduli the nature of the stress singularity at a crack tip would be identical to that of a homogeneous solid". And, Erdogan [3] stated " . . . if the crack is embedded into a nonhomogeneous medium with smoothly varying elastic properties the square root nature of the stress singularity *seems* to remain unchanged". It will be shown that regardless of the functional form of the modulus variation, an $r^{-1/2}$ stress and strain singularity exists at the crack tip. The angular variation of the singular stress field and the associated displacements around a crack tip in a nonhomogeneous material are shown to be exactly the same as the angular variation in a homogeneous material.

The literature concerned with analytical determination of stress intensity factors in nonhomogeneous materials whose elastic moduli vary smoothly is quite sparse, particularly for mode *I* and mode *II* deformation states. All solutions to date have addressed fracture of two-dimensional elastic media of infinite extent. The mode *I* stress intensity factor for an incompressible elastic body with a shear modulus which varies in the direction perpendicular to the crack line according to $\mu = \bar{\mu}(1 + \beta|y|)$ was studied by Rogers [4]. A singular integral equation was obtained which did not admit a closed-form solution. A variation of this problem was investigated by Gerasoulis [5]. The incompressibility assumption was relaxed and the shear modulus was taken to vary inversely as a function of distance from the crack line according to $\mu = \bar{\mu}/(1 + \beta|y|)$. The work by Delale [2] was the first to deal with the relatively more complicated problem of mode *I* deformation in the presence of a modulus variation in the direction parallel to the crack line. Young's modulus was given by $E = \bar{E} \exp(\beta x)$, while Poisson's ratio was constant. A singular integral equation was derived and then solved numerically to produce the stress intensity factor and crack surface displacement for a variety of load cases. Fabrikant [6] has analyzed a semi-infinite crack in a three-dimensional nonhomogeneous elastic body whose shear modulus varies according to a power law in the coordinate direction normal to the crack plane. Solutions for mode *II* cracks in nonhomogeneous materials were seemingly absent in the literature. Dhaliwal [4], Delale [8], and Erdogan [9] have analyzed crack problems in nonhomogeneous materials under mode *III* deformations. The analysis by Erdogan [9] is particularly interesting in that a problem where a shear modulus possessing a discontinuous derivative is studied. Furthermore, an analytical solution has not been obtained for the case of a continuously variable Poisson's ratio. The only prior direct numerical (as opposed to integral equations) work

related to fracture of nonhomogeneous materials of the type under discussion was by Atkinson [10]. A boundary integral equation crack tip analysis was executed to compute stress intensity factors in finite nonhomogeneous bodies subjected to mode *III* deformation.

Common features (or limitations) of all the prior analytical solutions for cracks in nonhomogeneous materials were the presence of an infinite domain and relatively simple functional forms for the modulus variation. In all cases the modulus variation was selected to render the governing partial differential equations mathematically tractable. The modulus variation is typically taken as a simple exponential or power-law along one of the Cartesian coordinate directions. Use of the finite element method is shown in this paper to overcome the limitations mentioned above. Realistic problems involving cracks require consideration of finite size effects. The finite element method can routinely handle difficult physical topologies. Secondly, the general procedures to be presented in the subsequent development do not restrict the functional form of the elastic modulus variation, including a variation in Poisson's ratio.

The organization of the paper is as follows. Section 2 contains a derivation of the stress and displacement fields near crack tips in arbitrary two-dimensional nonhomogeneous elastic bodies. Section 3 sets forth the necessary theoretical basis for determining stress intensity factors in nonhomogeneous cracked bodies via domain-independent integrals. An extension of the standard J integral (Rice [11]), which requires that a domain integral be appended to the usual line integral term, is developed. Simple relationships are shown to exist between the new $\boldsymbol{J}^*$ vector and the mode I and II stress intensity factors. Section 4 contains several numerical examples which verify the theoretical and computational issues described herein.

2. Stress analysis of cracks in nonhomogeneous elastic solids

A direct way to ascertain the nature of the near-tip fields in a cracked body is the eigenfunction expansion technique due to Williams [12]. This procedure has been widely exploited in fracture mechanics analysis of homogeneous bodies in the past. An extension of this conventional procedure is used to establish the general form of the stress and displacement fields near a crack tip in a nonhomogeneous material. Figure 1 shows a crack embedded in a two-dimensional nonhomogeneous elastic body. Cartesian and cylindrical coordinate systems have been fixed at the crack tip. Applied tractions and/or specified displacements on the boundary of the body are shown schematically, and are assumed to result in a state of generalized plane stress or plane strain. Body forces are neglected, and crack faces are assumed traction-free.

The stress equilibrium equations are satisfied identically by an Airy stress function $\phi(r, \theta)$ such that

$$\sigma_{rr} = \frac{1}{r}\frac{\partial \phi}{\partial r} + \frac{1}{r^2}\frac{\partial^2 \phi}{\partial \theta^2}, \qquad \sigma_{\theta\theta} = \frac{\partial^2 \phi}{\partial r^2}, \qquad \sigma_{r\theta} = -\frac{\partial}{\partial r}\left(\frac{1}{r}\frac{\partial \phi}{\partial \theta}\right) \tag{1}$$

where σ_{rr}, $\sigma_{\theta\theta}$, and $\sigma_{r\theta}$ are the cylindrical components of the stress tensor. The strain compatibility equation expressed in terms of cylindrical coordinates is

$$\frac{1}{r^2}\frac{\partial^2 \varepsilon_{rr}}{\partial \theta^2} + \frac{\partial^2 \varepsilon_{\theta\theta}}{\partial r^2} - \frac{1}{r}\frac{\partial \varepsilon_{rr}}{\partial r} + \frac{2}{r}\frac{\partial \varepsilon_{\theta\theta}}{\partial r} = \frac{2}{r}\frac{\partial^2 \varepsilon_{r\theta}}{\partial r \partial \theta} + \frac{2}{r^2}\frac{\partial \varepsilon_{r\theta}}{\partial \theta}. \tag{2}$$

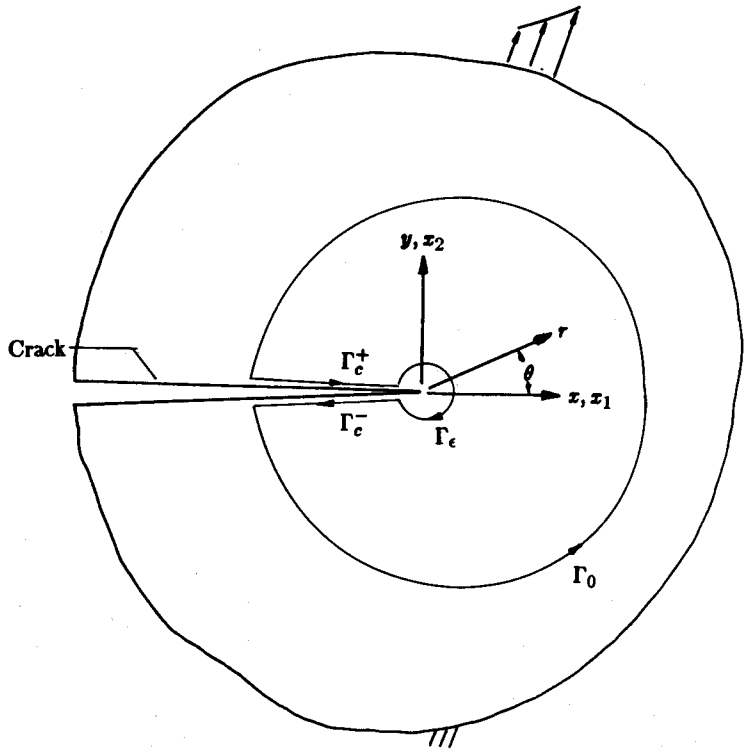

Fig. 1. Schematic of cracked body.

The elastic moduli E and ν are assumed to vary with position according to

$$E = E(r, \theta), \qquad \nu = \nu(r, \theta) \tag{3}$$

where $E(r, \theta)$ and $\nu(r, \theta)$ are continuous, bounded, and generally differentiable functions. Furthermore, it is required that $E > 0$ and $-1 < \nu < \frac{1}{2}$ everywhere in the domain. When the stress-strain relations and (1) are substituted into (2), the following equation governing the stress function ϕ for generalized plane stress conditions is obtained

$$\begin{aligned}
\nabla^4\phi &+ \left[\frac{2}{E^2}\left(\frac{\partial E}{\partial r}\right)^2 - \frac{1}{E}\frac{\partial^2 E}{\partial r^2}\right]\left[\frac{\partial^2\phi}{\partial r^2} - \nu\left(\frac{1}{r}\frac{\partial\phi}{\partial r} + \frac{1}{r^2}\frac{\partial^2\phi}{\partial\theta^2}\right)\right] \\
&+ \left[\frac{2}{E^2}\left(\frac{\partial E}{\partial \theta}\right)^2 - \frac{1}{E}\frac{\partial^2 E}{\partial \theta^2}\right]\left[\frac{1}{r^3}\frac{\partial\phi}{\partial r} + \frac{1}{r^4}\frac{\partial^2\phi}{\partial\theta^2} - \frac{\nu}{r^2}\frac{\partial^2\phi}{\partial r^2}\right] \\
&+ \frac{1}{E}\frac{\partial E}{\partial r}\left[-2\frac{\partial^3\phi}{\partial r^3} - \frac{2}{r}\frac{\partial^2\phi}{\partial r^2} + \frac{1}{r^3}\frac{\partial^2\phi}{\partial\theta^2} + \frac{1}{r^2}\frac{\partial\phi}{\partial r} + \nu\left(\frac{2}{r^2}\frac{\partial^3\phi}{\partial r\partial\theta^2} + \frac{1}{r}\frac{\partial^2\phi}{\partial r^2} - \frac{2}{r^3}\frac{\partial^2\phi}{\partial\theta^2}\right)\right] \\
&+ \frac{1}{E}\frac{\partial E}{\partial \theta}\left[\frac{2\nu}{r^2}\frac{\partial^3\phi}{\partial r^2\partial\theta} - \frac{2}{r^4}\frac{\partial^3\phi}{\partial\theta^3} - \frac{2}{r^3}\frac{\partial^2\phi}{\partial r\partial\theta}\right]
\end{aligned}$$

$$+\left[2\frac{(1+\nu)}{E^2}\frac{\partial E}{\partial r}\frac{\partial E}{\partial \theta}-\frac{(1+\nu)}{E}\frac{\partial^2 E}{\partial r\partial\theta}\right]\left[\frac{2}{r^2}\frac{\partial^2\phi}{\partial r\partial\theta}-\frac{2}{r^3}\frac{\partial\phi}{\partial\theta}\right]$$

$$+\frac{(1+\nu)}{E}\left[\frac{\partial E}{\partial r}\left(-\frac{2}{r^2}\frac{\partial^3\phi}{\partial r\partial\theta^2}+\frac{2}{r^3}\frac{\partial^2\phi}{\partial\theta^2}\right)+\frac{\partial E}{\partial\theta}\left(-\frac{2}{r^2}\frac{\partial^3\phi}{\partial r^2\partial\theta}+\frac{2}{r^3}\frac{\partial^2\phi}{\partial r\partial\theta}-\frac{2}{r^4}\frac{\partial\phi}{\partial\theta}\right)\right]$$

$$-\frac{\partial^2 v}{\partial r^2}\left[\frac{1}{r}\frac{\partial\phi}{\partial r}+\frac{1}{r^2}\frac{\partial^2\phi}{\partial\theta^2}\right]-\frac{\partial^2 v}{\partial r\partial\theta}\left[\frac{2}{r^3}\frac{\partial\phi}{\partial\theta}-\frac{2}{r^2}\frac{\partial^2\phi}{\partial r\partial\theta}\right]-\frac{\partial^2 v}{\partial\theta^2}\left[\frac{1}{r^2}\frac{\partial^2\phi}{\partial r^2}\right]$$

$$-\frac{\partial v}{\partial r}\left[\frac{1}{r}\frac{\partial^2\phi}{\partial r^2}\right]-\frac{\partial v}{\partial\theta}\left[-\frac{1}{r^2}\frac{\partial^3\phi}{\partial r^2\partial\theta}+\frac{2}{r^3}\frac{\partial^2\phi}{\partial r\partial\theta}-\frac{2}{r^4}\frac{\partial\phi}{\partial\theta}\right]$$

$$+\frac{2}{E}\frac{\partial E}{\partial r}\frac{\partial v}{\partial r}\left[\frac{1}{r^2}\frac{\partial^2\phi}{\partial\theta^2}+\frac{1}{r}\frac{\partial\phi}{\partial r}\right]+\frac{1}{E}\frac{\partial E}{\partial r}\frac{\partial v}{\partial\theta}\left[-\frac{2}{r^2}\frac{\partial^2\phi}{\partial r\partial\theta}+\frac{2}{r^3}\frac{\partial\phi}{\partial\theta}\right]$$

$$+\frac{1}{E}\frac{\partial E}{\partial\theta}\frac{\partial v}{\partial r}\left[-\frac{2}{r^2}\frac{\partial^2\phi}{\partial r\partial\theta}+\frac{2}{r^3}\frac{\partial\phi}{\partial\theta}\right]+\frac{1}{E}\frac{\partial E}{\partial\theta}\frac{\partial v}{\partial\theta}\left[\frac{1}{r^2}\frac{\partial^2\phi}{\partial r^2}\right]$$

$$= 0. \tag{4}$$

The first term in the governing equation for ϕ involves the biharmonic operator just as in the case of a homogeneous material, while all remaining terms include spatial derivatives of the elastic moduli E and ν. The corresponding relation for plane strain will not be written out here, but it is obtained by replacing E and ν by $E/(1-\nu^2)$ and $\nu/(1-\nu)$, respectively.

The next task is to obtain a solution for the stress function given the governing equation. A separation of variables method is applicable, with an appropriate structure of the stress function expressed as

$$\phi(r,\theta) = r^{\lambda+1}F(\theta)+r^{\lambda+2}G(\theta)+r^{\lambda+3}H(\theta)+O(r^{\lambda+4})+\ldots \tag{5}$$

where λ is an unspecified positive parameter. The functions F, G, and H are unknown at this stage. The ellipses indicate an infinite sequence of terms whose form is apparent given the pattern of the first few terms in (5). Because the elastic moduli are given by continuous and differentiable functions, they can be represented by a Maclaurin series expansion about the crack tip position ($r = 0$). The expansion for Young's modulus is written as

$$E(r,\theta) = E_0\left(1+rE_1(\theta)+\frac{r^2}{2}E_2(\theta)+O(r^3)+\ldots\right) \tag{6}$$

where E_0 = constant, and $E_1(\theta)$, $E_2(\theta)$ are smooth, bounded functions of θ. The expressions required for E^{-1} and E^{-2} are formed in terms of E_0, $E_1(\theta)$, etc., and $E_2(\theta)$ via the binomial expansion. The Maclaurin series expansion for Poisson's ratio can be written in a similar fashion to E. In order to lessen the algebraic burden during this presentation, it will henceforth be assumed that Poisson's ratio is constant. This simplification does not alter any of the final conclusions of the present analysis. Upon substituting Eqns. (5) and (6) into (4), it

is found that the assumed form for the stress function will satisfy the governing equation if

$$\begin{aligned}&[L^1_{\lambda+1}(F)]r^{\lambda-3} + [L^1_{\lambda+2}(G) - E_1''(\theta)L^3_{\lambda+1}(F) + E_1(\theta)L^4_{\lambda+1}(F)\\&\quad + E_1'(\theta)L^5_{\lambda+1}(F) - (1+\nu)(E_1'(\theta)L^6_{\lambda+1}(F) - E_1(\theta)L^7_{\lambda+1}(F) - E_1'(\theta)L^8_{\lambda+1}(F))]r^{\lambda-2}\\&\quad + [L^1_{\lambda+3}(H) + f(E_1(\theta), E_2(\theta), \nu, F(\theta), G(\theta))]r^{\lambda-1} + O(r^{\lambda}) + \cdots = 0 \qquad (7)\end{aligned}$$

where $f(\ldots)$ indicates a function of the arguments inside the parentheses. Terms have been grouped to multiply $r^{\lambda-3}$, $r^{\lambda-2}$, $r^{\lambda-1}$, ... The symbols $L^m_{\lambda+n}(\ )$ indicate differential operators which act on the functions F, G, and H. The explicit form of these operators is given in the Appendix.

Equation (7) is satisfied only if each of the functions inside the brackets [ ] are set equal to zero, leading to the following system of ordinary differential equations (ODE's) which will subsequently permit a determination of F, G, and H.

$$L^1_{\lambda+1}(F) = 0 \qquad (8)$$

$$\begin{aligned}L^1_{\lambda+2}(G) &= E_1''(\theta)L^3_{\lambda+1}(F) - E_1(\theta)L^4_{\lambda+1}(F) - E_1'(\theta)L^5_{\lambda+1}(F)\\&\quad + (1+\nu)(E_1'(\theta)L^6_{\lambda+1}(F) - E_1(\theta)L^7_{\lambda+1}(F) - E_1'(\theta)L^8_{\lambda+1}(F)) \qquad (9)\end{aligned}$$

$$L^1_{\lambda+3}(H) = -f(E_1(\theta), E_2(\theta), \nu, F(\theta), G(\theta)). \qquad (10)$$

Equation (8) is a fourth order, linear, homogeneous ODE for the unknown function $F(\theta)$. Equations (9) and (10) are fourth order, linear, nonhomogeneous ODE's and must be solved accordingly for the unknown functions $G(\theta)$ and $H(\theta)$, respectively. These three equations will be considered in turn. The general solution of (8) is

$$\begin{aligned}F(\theta) &= A\cos[(\lambda+1)\theta] + B\sin[(\lambda+1)\theta]\\&\quad + C\cos[(\lambda-1)\theta] + D\sin[(\lambda-1)\theta] \qquad (11)\end{aligned}$$

where A, B, C, D are unspecified constants. The traction-free crack surface boundary conditions which must be imposed are

$$\sigma_{\theta\theta}(r, \pm\pi) = \sigma_{r\theta}(r, \pm\pi) = 0 \qquad (12)$$

Imposition of these conditions leads to an eigenproblem requiring $\lambda_n = n/2$, $n = 1, 2, \ldots, \infty$. Additionally, the constants A and B are expressible in terms of C and D. The eigenfunctions $F_n(\theta)$ are given by

$$\begin{aligned}F_n(\theta) &= C_n\left\{\cos\left[\left(\frac{n}{2}-1\right)(\theta+\pi)\right] - \cos\left[\left(\frac{n}{2}+1\right)(\theta+\pi)\right]\right\}\\&\quad + D_n\left\{\sin\left[\left(\frac{n}{2}-1\right)(\theta+\pi)\right] - \frac{n-2}{n+2}\sin\left[\left(\frac{n}{2}+1\right)(\theta+\pi)\right]\right\}. \qquad (13)\end{aligned}$$

The next task is to investigate the character of the function $G(\theta)$. This function must satisfy the ODE given by (9), whose general solution is comprised of the sum of a particular and complementary solution, i.e.,

$$G_n(\theta) = G_n^p(\theta) + G_n^c(\theta) \tag{14}$$

The particular solutions $G_n^p(\theta)$ depend on the functions $F_n(\theta)$ and the specific material nonhomogeneity, as evidenced by (9). The complementary solution is of the form

$$G_n^c(\theta) = H_n \cos\left(\frac{n}{2} + 2\right)\theta + I_n \sin\left(\frac{n}{2} + 2\right)\theta + J_n \cos\frac{n}{2}\theta + K_n \sin\frac{n}{2}\theta \tag{15}$$

where H_n, I_n, J_n, and K_n ($n = 1, 2, \ldots, \infty$) are unspecified constants. The particular solutions cannot be obtained until an explicit form of the elastic moduli variation is chosen. Even then it would not be a routine matter to determine $G_n^p(\theta)$. The method of variation of parameters would be an appropriate technique in this situation because the form of the homogeneous solution is known (Boyce [13]). Nevertheless, once $G_n^p(\theta)$ is available the constants H_n thru K_n could be determined by imposing (12). A similar procedure would be followed to determine $H(\theta)$. Fortunately, for the intents herein, explicit knowledge of the forms of $G(\theta)$ and $H(\theta)$ is not necessary. This fact will become apparent in the subsequent development.

The components of stress are calculated from the following formulas, which follow from linear superposition of the eigensolutions for $F(\theta)$, $G(\theta)$, and $H(\theta)$

$$\sigma_{rr} = \sum_{n=1,2\ldots}^{\infty} \left\{ r^{(n/2)-1}\left[F_n'' + \left(\frac{n}{2} + 1\right)F_n\right] + r^{n/2}\left[G_n'' + \left(\frac{n}{2} + 2\right)G_n\right] + r^{(n/2)+1}\left[H_n'' + \left(\frac{n}{2} + 3\right)H_n\right] + O(r^{(n/2)+2}) + \ldots \right\} \tag{16}$$

$$\sigma_{\theta\theta} = \sum_{n=1,2\ldots}^{\infty} \left\{ r^{(n/2)-1}\left[\frac{n}{2}\left(\frac{n}{2} + 1\right)F_n\right] + r^{n/2}\left[\left(\frac{n}{2} + 1\right)\left(\frac{n}{2} + 2\right)G_n\right] + r^{(n/2)+1}\left[\left(\frac{n}{2} + 2\right)\left(\frac{n}{2} + 3\right)H_n\right] + O(r^{(n/2)+2}) + \ldots \right\} \tag{17}$$

$$\sigma_{r\theta} = \sum_{n=1,2\ldots}^{\infty} \left\{ r^{(n/2)-1}\left[-\frac{n}{2}F_n'\right] + r^{n/2}\left[-\left(\frac{n}{2} + 1\right)G_n'\right] + r^{(n/2)+1}\left[-\left(\frac{n}{2} + 2\right)H_n'\right] + O(r^{(n/2)+2}) + \ldots \right\}. \tag{18}$$

Only the leading term in the expressions for the components of stress, which is $O(r^{(n/2)-1})$, contributes to the components of stress which are singular as $r \to 0$. Because fracture criteria typically depend only on the character of the singular stress components (and sometimes

$O(1)$ terms), explicit determination of $G(\theta)$ and $H(\theta)$ is not necessary for the following reason. Since n takes on the values 1, 2, . . . , the leading terms in the expressions for the components of stress will have r raised to the powers $-1/2$, 0, 1/2, ... The second term in the expression for the components of stress ($O(r^{n/2})$) will have r raised to the powers 1/2, 1, 3/2, ... These terms are all bounded at the crack tip. Therefore, it is clear that all terms in these expressions that follow the $O(r^{n/2})$ term result in components of stress which are non-singular. Stress components referred to a Cartesian basis (x, y) will be given to conform with traditional presentations. Using (13) in Eqns. (16)–(18), making a coordinate transformation, and omitting terms $O(r^{1/2})$ and above, the following approximate expressions for the stress components are obtained

$$\sigma_{xx} \cong \frac{K_I}{(2\pi r)^{1/2}} f_{xx}^I(\theta) + \frac{K_{II}}{(2\pi r)^{1/2}} f_{xx}^{II}(\theta) + \sigma_{x0} + O(r^{1/2}) + \ldots \tag{19}$$

$$\sigma_{yy} \cong \frac{K_I}{(2\pi r)^{1/2}} f_{yy}^I(\theta) + \frac{K_{II}}{(2\pi r)^{1/2}} f_{yy}^{II}(\theta) + O(r^{1/2}) + \ldots \tag{20}$$

$$\sigma_{xy} \cong \frac{K_I}{(2\pi r)^{1/2}} f_{xy}^I(\theta) + \frac{K_{II}}{(2\pi r)^{1/2}} f_{xy}^{II}(\theta) + O(r^{1/2}) + \ldots \tag{21}$$

where the constants C_1, C_2, and D_1 have been redefined as

$$C_1 = \frac{K_{II}}{\sqrt{2\pi}}, \qquad C_2 = \frac{\sigma_{x0}}{4}, \qquad D_1 = \frac{-K_I}{\sqrt{2\pi}}. \tag{22}$$

The mode *I* and mode *II* stress intensity factors are designated K_I and K_{II}, respectively. The σ_{xx} stress component contains an $O(1)$ term, σ_{x0}, called the "nonsingular stress". This parameter has been associated with crack kinking phenomena. The ellipses designate a sequence of terms which are of successively higher degree in r. The symbols $f_{xx}^I, f_{xx}^{II}, f_{yy}^I$, etc. represent trigonometric functions of the angle θ and are given by Eftis [14].

The significant results of these calculations is that the nature of the stress singularity is precisely the same as the well-known form applicable to homogeneous materials, irrespective of the particular form of the Young's modulus variation. The terms in the series representation for the stresses proportional to $r^{-1/2}$ and r^0 are not affected by material nonhomogeneity. The degree of the singularity is preserved ($-1/2$) in the presence of nonhomogeneity, as well as the angular dependence given by f_{xx}^I, f_{xx}^{II}, etc. The angular variation of the components of stress which correspond to terms $O(r^{1/2})$ and higher ($r^1, r^{3/2}, \ldots$) do change due to material nonhomogeneity. The same general results are obtained if Poisson's ratio varies "smoothly" within the domain of the cracked body. In addition to depending on the geometry and loading of the cracked body, K_I and K_{II} will depend on the variation of the elastic moduli. However, this dependence cannot be ascertained by the eigenfunction expansion procedure. A method to accomplish this task will be discussed in Section 3. Additionally, a forthcoming paper will address the problem where the elastic moduli are given by continuous functions not necessarily possessing continuous derivatives.

The components of displacement are obtained by integrating the strain displacement relations. Only those terms in the series expansions for the displacements which dominate

near the crack tip are of immediate interest. The stress-strain relations and the series expansion for Young's modulus are used to derive the strain components in terms of the functions $F(\theta)$, $G(\theta)$, $H(\theta)$. After some manipulations, the expressions for the Cartesian components of displacement given in terms of the cylindrical coordinates (r, θ) appear as

$$u_x \cong \frac{K_I}{\mu_0}\left(\frac{r}{2\pi}\right)^{1/2} g_x^I(\theta) + \frac{K_{II}}{\mu_0}\left(\frac{r}{2\pi}\right)^{1/2} g_x^{II}(\theta) + u_{x0} - \omega_0 r \sin\theta$$

$$+ \frac{r}{2\mu_0}\{C_2(\kappa + 1)\cos\theta + D_2(\kappa + 1)\sin\theta\} + O(r^{3/2}) + \ldots \tag{23}$$

$$u_y \cong \frac{K_I}{\mu_0}\left(\frac{r}{2\pi}\right)^{1/2} g_y^I(\theta) + \frac{K_{II}}{\mu_0}\left(\frac{r}{2\pi}\right)^{1/2} g_y^{II}(\theta) + u_{y0} + \omega_0 r \cos\theta$$

$$+ \frac{r}{2\mu_0}\{C_2(\kappa - 3)\sin\theta - D_2(\kappa + 1)\cos\theta\} + O(r^{3/2}) + \ldots \tag{24}$$

where $\mu_0 = E_0/2(1 + \nu)$, and $\kappa = 3 - 4\nu$ for plane strain or $3 - \nu/1 + \nu$ for generalized plane stress. The constants u_{x0}, u_{y0}, and ω_0 are associated with rigid body displacements and rotations. The functions $g_x^I(\theta)$, $g_x^{II}(\theta)$, etc. are given in [14]. The elastic modulus appearing in the leading term of (23) and (24) is μ_0, the value of the shear modulus at the crack tip. Again, the nature of the near tip displacement field is the same as for the homogeneous material. The terms $O(r^{3/2})$ and above do not exhibit the same spatial dependence as the corresponding terms for a homogeneous material. In summary, the form of the terms proportional to $r^{1/2}$, r^0 and r are "universal" in that they do not depend on variation of the elastic moduli.

The analysis presented above did not include a possible spatial variation in Poisson's ratio. If such a variation were considered, the following substitutions would be made in (23) and (24); $\mu_0 = E_0/2(1 + \nu_0)$ and $\kappa = \kappa_0$.

3. Domain-independent integral for nonhomogeneous materials

By far the most common concern pertaining to linear elastic fracture mechanics analysis is the accurate prediction of stress intensity factors in arbitrarily shaped cracked bodies. Rarely can a complete solution for a finite body containing a crack be found using analytical methods. Numerical techniques (e.g. finite elements, finite differences, boundary integrals, etc.) are generally necessary to compute requisite field quantities. After stress and displacement fields have been obtained, two choices exist for extracting the stress intensity factors from the numerical data. They can be calculated "directly" using the computed displacements and/or stresses near the crack tip. The second choice involves calculating the stress intensity factors "indirectly" via path independent integrals. The motivation for using such integrals is that evaluation of near tip field quantities can be avoided, yet the value of the integrals is related to the crack tip stress intensity factors. A balance law associated with linear elasticity will be used to derive integrals which prove useful for computing stress

intensity factors in nonhomogeneous bodies containing cracks. These integrals are also shown to be related to the energetics of the fracture process in certain circumstances.

There are a number of methods to generate path-independent integrals in elasticity theory. The most elegant method is based on Noether's theorem (Knowles [15]). For the present purpose, a simple and direct approach is taken which extends some of the classical work of Eshelby [16]. A nonhomogeneous elastic body subjected to a two-dimensional deformation field (plane strain, generalized plane stress) possesses a strain energy density function W defined by

$$W = W(\varepsilon_{ij}, x_i) \qquad \text{where} \qquad \sigma_{ij} = \frac{\partial W}{\partial \varepsilon_{ij}} \qquad (i, j = 1, 2). \tag{25}$$

Note that when the material is homogeneous, the strain energy function will be $W = W(\varepsilon_{ij})$. To derive a balance law, the gradient of W is formed, i.e.,

$$\frac{\partial W}{\partial x_k} = \frac{\partial W}{\partial \varepsilon_{ij}} \frac{\partial \varepsilon_{ij}}{x_k} + \left(\frac{\partial W}{\partial x_k}\right)_{\text{expl}} \tag{26}$$

where the "explicit" derivative of W is defined by

$$\left(\frac{\partial W}{\partial x_k}\right)_{\text{expl}} = \frac{\partial}{\partial x_k} W(\varepsilon_{ij}, x_i)|_{\varepsilon_{ij} = \text{const}, x_m = \text{const for} m \neq k}. \tag{27}$$

Equation (26) becomes

$$W_{,k} = \sigma_{ij} \varepsilon_{ij,k} + (W_{,k})_{\text{expl}}. \tag{28}$$

Using the symmetry properties of the stress tensor, the linearized strain-displacement relations, and the equilibrium equations, it follows that

$$(W\delta_{jk} - \sigma_{ij} u_{i,k})_{,j} - (W_{,k})_{\text{expl}} = 0 \tag{29}$$

where δ_{jk} is the Kronecker delta. This vector equation represents a *balance law*, valid pointwise, for a nonhomogeneous elastic body (not necessarily isotropic).

An integral form of (29) proves necessary for application in computational work. A simple closed curve Γ in the x_1, x_2 plane is introduced along with the domain Ω which it encloses. By integrating (29) over the domain Ω and applying the divergence theorem, the following formula results

$$\oint_\Gamma (Wn_k - \sigma_{ij} n_j u_{i,k}) d\Gamma - \int_\Omega (W_{,k})_{\text{expl}} d\Omega = 0 \tag{30}$$

where n_j is a measure number of the outward unit normal vector to Γ.

For a linear elastic nonhomogeneous material the strain energy function is of the form

$$W = \tfrac{1}{2} c_{prst}(x_1, x_2) u_{p,r} u_{s,t} \tag{31}$$

where c_{prst} denotes the elasticity tensor. For an isotropic nonhomogeneous material, the "explicit" derivative of W is then

$$(W_{,k})_{\text{expl}} = \tfrac{1}{2}[\lambda_{,k}\delta_{pr}\delta_{st} + \mu_{,k}(\delta_{ps}\delta_{rt} + \delta_{pt}\delta_{rs})]u_{p,r}u_{s,t} \tag{32}$$

where λ and μ are the Lame' moduli.

So far no mention of a crack in the region Ω has been made. However, in applying the divergence theorem it was tacitly assumed that field quantities were continuous, bounded, and generally differentiable on Ω. Since the stress and strain fields are singular at a crack tip, and therefore unbounded, the region Ω referred to in (30) must not contain a crack tip. In order to derive an integral expression which is valid in the presence of a crack tip, a rather special region Ω must be considered. Figure 1 shows a crack located in a two-dimensional body of arbitrary shape. Tractions are permitted to act on the crack surfaces. The horseshoe shaped region Ω (free of singularities) is bounded by a closed curve Γ composed of segments Γ_0, Γ_c^+, Γ_ε, Γ_c^- as shown. The region between Γ_ε and the crack surfaces is Ω_ε. The region Ω_0 is defined as $\Omega + \Omega_\varepsilon$. The divergence theorem can be applied in the region Ω, because the singular fields at the crack tip are excluded. Equation (30) can be used to write

$$\oint_{\Gamma_0} b_k d\Gamma + \int_{\Gamma_c^+} b_k d\Gamma + \oint_{\Gamma_\varepsilon} b_k d\Gamma + \int_{\Gamma_c^-} b_k d\Gamma - \int_{\Omega} (W_{,k})_{\text{expl}} d\Omega = 0 \tag{33}$$

where

$$b_k = Wn_k - \sigma_{ij}n_j u_{i,k}. \tag{34}$$

If the direction of integration is reversed on the third term of (33), and the region Ω is decomposed into $\Omega_0 - \Omega_\varepsilon$ it follows that

$$\oint_{\Gamma_0} b_k d\Gamma - \int_{\Omega_0} (W_{,k})_{\text{expl}} d\Omega + \int_{\Gamma_c^+} b_k d\Gamma + \int_{\Gamma_c^-} b_k d\Gamma = \oint_{\Gamma_\varepsilon} b_k d\Gamma - \int_{\Omega_\varepsilon} (W_{,k})_{\text{expl}} d\Omega. \tag{35}$$

A vector $\boldsymbol{J}^*$ is introduced whose measure numbers are defined by the right-hand side of (35)

$$J_k^* \equiv \lim_{\Gamma_\varepsilon \to 0} \left[\oint_{\Gamma_\varepsilon} b_k d\Gamma - \int_{\Omega_\varepsilon} (W_{,k})_{\text{expl}} d\Omega \right] \tag{36}$$

As the loop Γ_ε is shrunk onto the crack tip, the domain integral in (36) vanishes, for the following reason. Field quantities are assumed to be expressed in terms of a cylindrical coordinate system whose origin is fixed at the crack tip. Derivatives of the elastic moduli are assumed to be bounded at the crack tip, i.e., $\lambda_{,k}$ and $\mu_{,k}$ are $O(r^\alpha)$, where $\alpha \geqslant 0$. Therefore, near the crack tip, $(W_{,k})_{\text{expl}}$ is $O(r^{-1+\alpha})$, and the domain integral vanishes in the limit. Then (35) and (36) can be combined to produce

$$\begin{aligned} J_k^* &\equiv \lim_{\Gamma_\varepsilon \to 0} \oint_{\Gamma_\varepsilon} [Wn_k - \sigma_{ij}n_j u_{i,k}] d\Gamma \\ &= \lim_{\Gamma_\varepsilon \to 0} \left\{ \oint_{\Gamma_0} [Wn_k - \sigma_{ij}n_j u_{i,k}] d\Gamma - \int_{\Omega_0} (W_{,k})_{\text{expl}} d\Omega \right. \\ &\quad \left. + \int_{\Gamma_c^+} [Wn_k - \sigma_{ij}n_j u_{i,k}] d\Gamma + \int_{\Gamma_c^-} [Wn_k - \sigma_{ij}n_j u_{i,k}] d\Gamma \right\}. \end{aligned} \tag{37}$$

The J_k^* integrals expressed in terms of Γ_0, Ω_0, Γ_c^+, Γ_c^- are clearly domain-independent. It is convenient to combine the two terms involving integrations along the crack faces, and simply call the associated path of integration Γ_c, understanding that quantities must still be evaluated on both the top and bottom crack surfaces. In order to combine these two terms, the path Γ_0 must intersect the top and bottom crack faces at points which are the same distance from the crack tip, as shown in Fig. 1. If the traction vector $\boldsymbol{t}$ is introduced, whose measure numbers are $t_i = \sigma_{ij} n_j$, (37) becomes

$$J_k^* = \lim_{\Gamma_\varepsilon \to 0} \left\{ \oint_{\Gamma_0} [W n_k - \sigma_{ij} n_j u_{i,k}] d\Gamma - \int_{\Omega_0} (W_{,k})_{\text{expl}} d\Omega \right.$$

$$\left. + \int_{\Gamma_c} ([W^+ - W^-] n_k^+ - [t_i^+ u_{i,k}^+ - t_i^- u_{i,k}^-]) \right\} d\Gamma \tag{38}$$

where the $(+)$ and $(-)$ refer to the upper and lower crack faces, and $n_k^+ = -n_k^-$ is the measure number of the outward unit normal vector to Γ_c^+. The notation $[W^+ - W^-]$ denotes the discontinuity (or "jump") in the strain energy density across the crack opening.

The presence of the material nonhomogeneity is seen to affect the standard J integral by requiring the addition of a domain integral term. This certainly detracts from the economy and simplicity of the standard J line integral. The domain integral contribution to J_k^* requires substantially more computational effort to evaluate than the line integral contribution. Nevertheless, the J_k^* integrals are a useful computational tool, and will be shown to have a physical interpretation as well.

A fracture criterion which has proved useful in studying crack extension is that based on the energy release rate. This criterion for fracture states that crack growth can occur only if the energy required to create new crack surfaces is available as stored elastic energy, or potential energy in externally applied tractions. The energy flow to the crack tip measured as a change in energy per unit crack extension per unit thickness is denoted by G. The approach taken in this section to generate an expression for G in a nonhomogeneous body will use some results of a prior analysis by Freund [17], who derived the energy release rate for a dynamically extending crack. Accounting for dynamic effects is not essential in treating the quasi-static crack extension process being studied here, but provides a very systematic way to derive the energy release rate expression.

The crack tip is assumed to be extending in a self-similar manner along the x_1 axis at time t, and the measure number of the crack tip velocity vector v is given by v_1. The small loop Γ_ε surrounding the crack tip is assumed to translate rigidly with it. The other segments of the boundary (Γ_0, Γ_c^+, Γ_c^-) are fixed in space. The tractions on these boundary segments are assumed to remain constant during crack extension (fixed-load conditions). Freund [17] showed that the energy absorption rate F, measured as a change in energy per unit thickness per unit time is

$$F = \oint_{\Gamma_\varepsilon} [\sigma_{ij} n_j \dot{u}_i + \tfrac{1}{2} \sigma_{ij} u_{i,j} v_1 n_1 + \tfrac{1}{2} \varrho \dot{u}_i \dot{u}_i v_1 n_1] d\Gamma \tag{39}$$

where the superposed dot indicates a time derivative, and ϱ designates the mass density. It is straightforward to verify that this expression is valid for a nonhomogeneous elastic solid.

Field quantities obey the "transport assumption" (Ehrlacher [18]) near the tip of an extending crack, i.e.

$$\frac{\partial(\ )}{\partial t} = -v_1 \frac{\partial(\ )}{\partial x_1}.$$

Given this fact, (39) becomes

$$F = v_1 \oint_{\Gamma_\varepsilon} \{[\tfrac{1}{2}\sigma_{ij}u_{i,j} + \tfrac{1}{2}\varrho\dot{u}_i\dot{u}_i]n_1 - \sigma_{ij}n_j u_{i,1}\}d\Gamma \tag{40}$$

In the case of quasi-static crack extension, the term containing ϱ tends to zero due to the absence of inertia effects. The energy release rate G is equal to F/v_1. Therefore

$$G = \oint_{\Gamma_\varepsilon} (Wn_1 - \sigma_{ij}n_j u_{i,1})d\Gamma = J_1^* \tag{41}$$

Equation (41) expresses the fact that J_1^* has a clear and precise physical meaning. J_2^* has a non-zero value in general, but apparently lacks a physical interpretation. The energy release rate G can also be expressed in terms of a remote path Γ_0 and associated domain Ω_0 by employing (38).

Another viewpoint regarding the physical interpretation of the J_1^* integral is possible. While the prior development considered the local energy release rate (at the crack tip), it is also feasible to associate J_k^* with a global energy release rate. It is easily shown that

$$J_1^* = \frac{\partial U}{\partial l} \tag{42}$$

where U is the total strain energy contained in the cracked body, while l is the instantaneous crack length.

The J_k integrals are directly related to the crack tip stress intensity factors. When employing cylindrical coordinates r and θ at the crack tip, as shown in Fig. 1, the stresses have been shown to be dominated by an inverse square root dependence on r, as given by (19)–(21). The corresponding displacements are dominated by a square root dependence on r, with explicit expressions given by (23) and (24). The J_k^* integrals defined by means of (36) can be evaluated using these expressions for the stress and displacement fields, taking Γ_ε to be a smaller circular loop of radius ε centered at the crack tip. The J_k^* integrals are sensitive only to the singular stress fields ($O(r^{-1/2})$) and the corresponding displacement fields ($O(r^{1/2})$), and therefore none of the higher order terms in the series expansions for the stresses and displacement contribute. It can be shown that

$$J_1^* = \frac{1}{E_0}(K_I^2 + K_{II}^2) \qquad J_2^* = \frac{1}{E_0}(-2K_IK_{II}) \quad \text{generalized plane stress} \tag{43}$$

$$= \frac{1 - \nu_0^2}{E_0}(K_I^2 + K_{II}^2) \qquad = \frac{1 - \nu_0^2}{E_0}(-2K_IK_{II}) \quad \text{plane strain} \tag{44}$$

where E_0 and ν_0 are the values of Young's modulus and Poisson's ratio at the crack tip. These formulas are identical in structure to the well-known relations valid for homogeneous materials (Herrmann [19]). The utility of the formulas derived in this section will now be illustrated by means of numerical examples.

4. Numerical results

The main purpose of this section is to demonstrate the viability of using the J_k^* integrals to compute stress intensity factors in cracked nonhomogeneous bodies. It is recognized that the stress intensity factors may also be computed directly from the near tip asymptotic formulas for displacement. In the third example problem results are presented based on computations of this type.

(a) *Center crack in a plate*

The first example problem considered is depicted in Fig. 2. A through crack of length $2a$ is situated in a finite two-dimensional plate. Young's modulus is an exponential function of x_1, while Poisson's ratio is constant. Delale [2] has reported results pertaining to an infinite plate with such a modulus variation. Stress intensity factors were computed after numerical solution of a singular integral equation. These results provide a means of validating finite element procedures which employ the J_k* integrals to determine the stress intensity factors in nonhomogeneous cracked bodies. The finite element mesh shown in Fig. 2 would generally be regarded as "coarse" for a typical fracture mechanics problem. A finite element model obviously cannot represent the infinite domains addressed in the analysis by Delale [2], but as long as the ratios a/W and a/L are kept relatively small, the approximation is quite acceptable. Eight-node serendipity quadrilateral elements were used over most of the mesh, while at each crack tip, quadrilateral elements were collapsed to form six-node triangles. These tip elements were arranged in the quarter-point configuration to properly account for the known $r^{-1/2}$ strain singularity. Three integration domains were selected to evaluate the J_1^* integral, as shown in Fig. 2. It should be noted that because $K_{II} = 0$ for this problem, computation of J_2^* was not necessary. Multiple domains were used to verify the path-independence property of the J_1^* integral, thereby providing a check on the numerical consistency of the results. The applied loading was such that $\sigma_{22}(x_1, 1) = \bar{\varepsilon}\bar{E}e^{\beta x_1}$. This stress distribution was obtained by applying nodal forces along the top edge of the mesh ($x_2 = 1$). This loading results in a uniform strain $\varepsilon_{22}(x_1, x_2) = \bar{\varepsilon}$ in a comparable *uncracked* structure. The following data were used for the finite element analysis: $a/W = 0.2$, $L/2W = 1.0$, $E(x_1) = \bar{E}e^{\beta x_1}$, $\bar{E} = 1.0\,\text{MPa}$, $\beta a = (0.0, 0.1, 0.25, 0.5, 0.75, 1.0)$, $\bar{\varepsilon} = 1.0$, $\nu = 0.3$, generalized plane stress, 2×2 Gauss quadrature. The stress intensity factor K_I v as computed by the formula $K_1 = \sqrt{E_0 J_1^*}$, where $E_0 = \bar{E}e^{\beta a}$. Table 1 compares the normalized stress intensity factor computed via the J_1^* integral with that reported in the paper by Delale [2]. The material nonhomogeneity is seen to elevate the stress intensity factor as compared with a homogeneous material for which $\beta a = 0$.

The second column in this table was formed in an attempt to "divide out" the effect of the finite size of the body. For a center crack in a homogeneous finite width sheet with

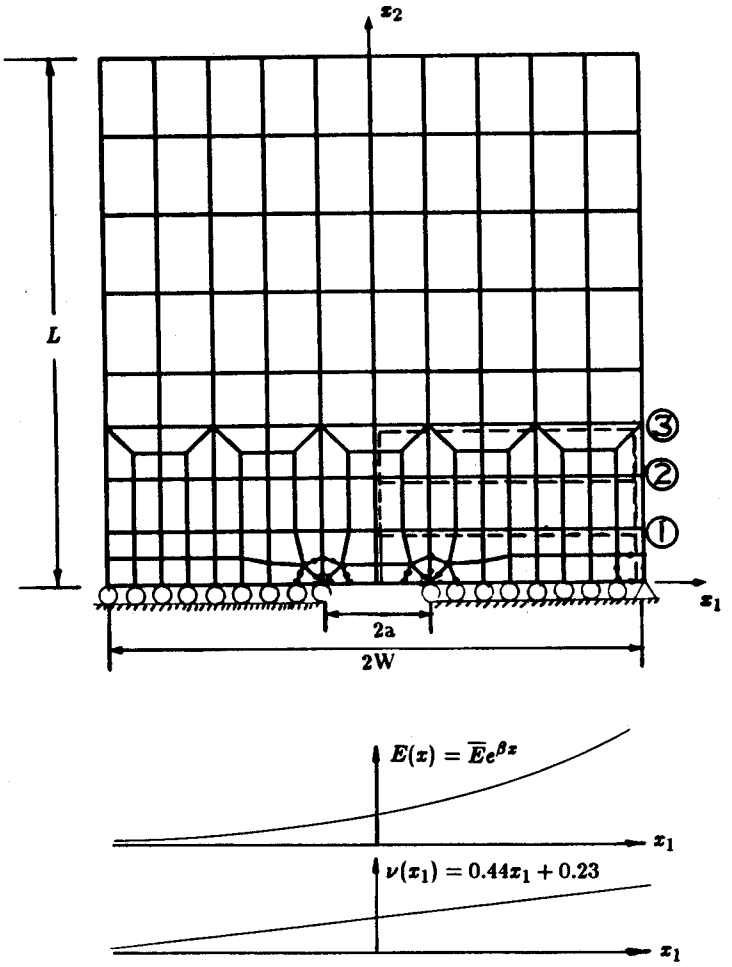

Fig. 2. Center cracked plate configuration and material property variation.

Table 1. Normalized stress intensity factor for a nonhomogeneous center cracked plate ($a/W = 0.2$)

βa	Present results (computed from J_1^*)		Delale [2]
	$K_I(\beta a)/\bar{\varepsilon}\bar{E}\sqrt{\pi a}$	$K_I(\beta a)/\bar{\varepsilon}\bar{E}\sqrt{\pi a}/1.031$	$K_I(\beta a)/\bar{\varepsilon}\bar{E}\sqrt{\pi a}$
0.00	1.031	1.000	1.000
0.10	1.112	1.078	1.078
0.25	1.252	1.215	1.202
0.50	1.531	1.485	1.435
0.75	1.823	1.769	1.713
1.00	2.089	2.026	2.048

$a/W = 0.2$, $K_I/\varepsilon_0\bar{E}\sqrt{\pi a} = 1.025$ (Broek [20]). This value represents the analytical (exact) solution for the homogeneous finite width sheet. The finite element analysis produced a value of 1.031, or less than a 1 percent difference compared with the exact solution. The factor 1.031 represents the so-called "back-face correction". By comparing the second and third column of Table 1, and noting the agreement between them, it appears that the back face correction factor is relatively unaffected by the material nonhomogeneity.

Table 2. J_1^* Integral partition for $\beta a = 0.5$

Domain No.	J_1^* (Line)	J_1^* (Domain)	J_1^*
1	0.816	0.594	0.222
2	1.390	1.166	0.224
3	1.954	1.730	0.224

Table 2 reports the relative contributions of the line integral term and the domain integral term to J_1^* ($=J_1^*$ (Line) $-$ J_1^* (Domain)) for $\beta a = 0.50$. J_1^* is seen to be virtually independent of the domain. Secondly, the magnitude of the domain integral contribution to J_1^* is an appreciable fraction of the line integral contribution, and certainly must be accounted for.

A two-dimensional crack problem in the presence of a continuously varying Poisson's ratio has never been dealt with analytically due to the intractable nature of the accompanying mathematics. However, this situation does not present any particular difficulty when using the finite element method. The mesh shown in Fig. 2 was employed to study this problem. Nodal forces were applied along the upper edge of the mesh such that $\sigma_{22}(x_1, 1.0) = \sigma_0 = 1.0\,\text{MPa}$. The variation of Poisson's ratio was assumed to be $\nu(x_1) = 0.44x_1 + 0.23$, which results in $\nu = 0.01$ on the left boundary and $\nu = 0.45$ on the right boundary. Young's modulus was taken to be a constant $E = 1.0\,\text{MPa}$. The normalized stress intensity factor $K_I/\sigma_0\sqrt{\pi a}$ was 1.029 for generalized plane stress, and 1.017 for plane strain conditions. The value of K_I computed (via J_1^*) for the homogeneous medium was 1.031, assuming generalized plane stress conditions (see Table 1). Therefore, a variation of Poisson's ratio in the direction of the crack line is seen to have negligible impact on the stress intensity factor.

(*b*) *Slanted crack in a plate*

The slanted crack in a two-dimensional elastic strip provides a mixed-mode loading situation which requires computation of both J_1^* and J_2^* in order to determine the stress intensity factors. Figure 3 shows the geometry, loading, and boundary conditions for the problem selected to serve as an example featuring mixed-mode loading. Given a homogeneous material, this configuration is nearly identical to one studied by Nishioka [21]. Eight-node serendipity quadrilateral elements were utilized over most of the mesh, while near the crack tip two element types were employed; (*i*) quarter-point, singular, isoparametric, six-node triangles, (*ii*) non-singular, isoparametric, six-node triangles. Three integration domains are also shown for evaluation of the J_k^* integrals. The following data was used for the finite element analysis: $a/W = 0.4\sqrt{2}$, $L/W = 2.0$, $E = 1.0\,\text{MPa}$, $\nu = 0.3$, generalized plane stress, 2×2 Gauss quadrature. Nodal forces were prescribed such that a state of uniform normal stress $\sigma_{2'2'}(x_1', 1) = \sigma_0 = 1.0\,\text{MPa}$ existed along the upper edge of the finite element model. Table 3 shows the normalized stress intensity factors computed via the J_k^* integrals. Details of the numerical procedure to separate the stress intensity factors from J_k^* will be given in a forthcoming paper (Eischen [22]). Bowie [23] reported results for this problem which were obtained using a highly accurate mapping technique. The present results are seen to agree very well with Bowie's results, regardless of the crack tip modeling. Bowie did not report results for the non-singular stress component σ_{x0}.

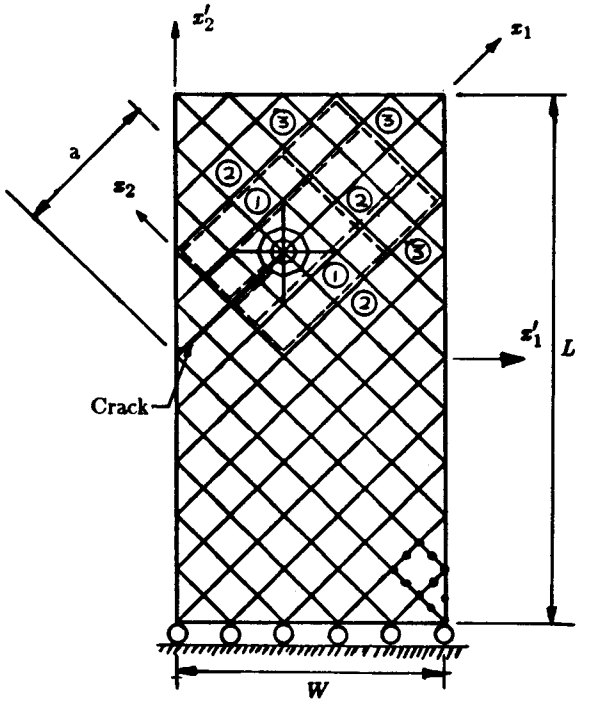

Fig. 3. Slanted crack in a plate configuration.

Table 3. Normalized stress intensity factors and non-singular stress component for a slanted crack computed using the J_k^* integrals (Homogeneous strip, $a/W = 0.4\sqrt{2}$, $L/W = 2.0$)

Crack tip elements	$K_I/\sigma_0\sqrt{\pi a}$	$K_{II}/\sigma_0\sqrt{\pi a}$	σ_{x0}/σ_0
Singular	1.438	0.605	0.822
Non-singular	1.410	0.625	0.621
Bowie [23]	1.450	0.620	N.A.

The slanted crack problem is now considered in the presence of a material nonhomogeneity. The Young's modulus was assumed to vary according to $E(x_1') = \bar{E}e^{\beta(x_1'-0.5)}$, where $\bar{E} = 1.0\,\text{MPa}$, $\beta a = 0.4\sqrt{2}$. Poisson's ratio was assumed constant throughout the domain. Nodal forces were prescribed along the upper edge of the model such that the normal stress varied according to $\sigma_{2'2'}(x_1', 1) = \bar{\varepsilon}\bar{E}e^{\beta(x_1'-0.5)}$, where $\bar{\varepsilon} = 1.0$. Table 4 shows the normalized stress intensity factors and non-singular stress component computed using the J_k^* integrals.

The results are seen to be virtually insensitive to the crack tip modeling. This is not the case when computing stress intensity factors directly from the nodal displacements.

Table 4. Normalized stress intensity factors and non-singular stress component for a slanted crack computed using the J_k^* integrals (Non-homogeneous strip, $\beta a = 0.4\sqrt{2}$, $a/W = 0.4\sqrt{2}$, $L/W = 2.0$)

Crack tip elements	$K_I/\bar{\varepsilon}\bar{E}\sqrt{\pi a}$	$K_{II}/\bar{\varepsilon}\bar{E}\sqrt{\pi a}$	$\sigma_{x0}/\bar{\varepsilon}\bar{E}$
Singular	0.984	0.395	0.588
Non-singular	0.967	0.409	0.460

(c) *Composite strip*

Fracture mechanics analyses of composite structures usually require consideration of the piecewise continuous nature of the elastic moduli comprising the structure. An approximate analysis of a composite structure is certainly possible by supposing that the material constituents possess smooth, but rapid variations in their elastic moduli. This class of materials falls within the scope of the theory and numerical analysis tools which have been developed in this paper. Such treatment of the material variation may in fact be more representative than conventional approaches given an interface where bonding or natural causes creates a diffuse variation of the elastic moduli.

The configuration under consideration in this section is depicted in Fig. 4. A crack of length a is located on the line $x_2 = 0$. A material interface exists on the line $x_1 = -0.1$, with $E = E_1$ for $x_1 > -0.1$, and $E = E_2$ for $x_1 < -0.1$. Poisson's ratio ν is constant throughout. For purposes of the present approximate analysis, Young's modulus $E(x_1)$ was assumed to vary smoothly across the natural material interface. The hyperbolic tangent function was utilized for this purpose. A nonhomogeneity parameter β was introduced to allow a more or less rapid variation of $E(x_1)$ across the interface. As $\beta a \to \infty$, a discontinuous jump in $E(x_1)$ occurs across the interface. Figure 4 shows the variation of $E(x_1)$ as a function of the parameter βa, for the case $E_1 = 1.0\,\text{MPa}$, $E_2 = 3.0\,\text{MPa}$. Nodal forces were prescribed along the upper edge of the finite element mesh resulting in a stress state given by $\sigma_{22}(x_1, 1) = \bar{\varepsilon}\bar{E}(x_1)$, corresponding to pure mode I loading. Three integration domains were

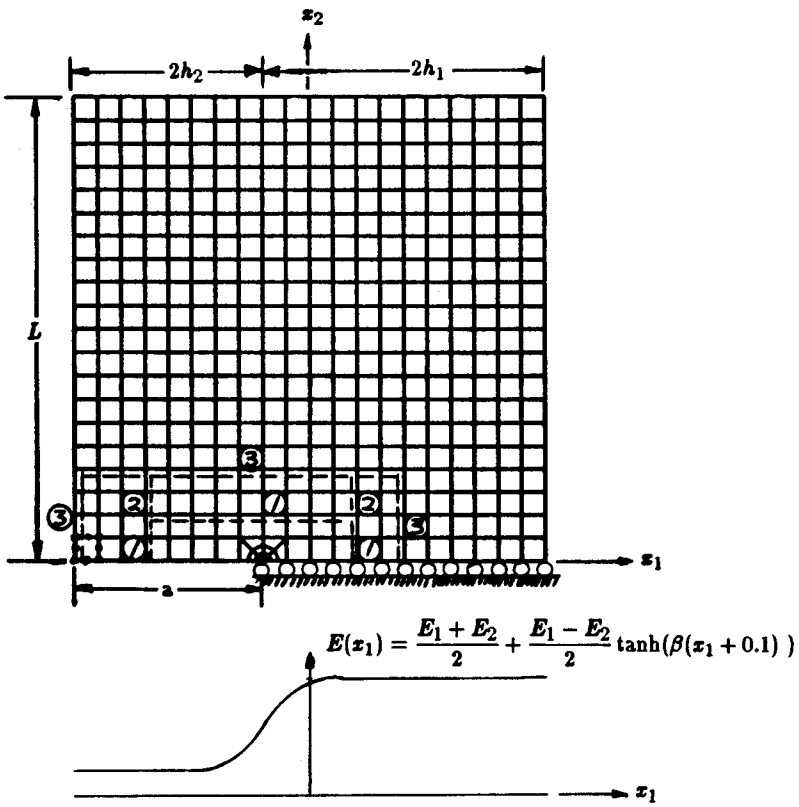

Fig. 4. Composite strip configuration and material property variation.

Table 5. Normalized stress intensity factor for composite strip configuration ($a/2h_1 = 0.67$, $h_1/h_2 = 1.5$, $L/2(h_1 + h_2) = 1.0$)

βa	$K_I/\bar{\varepsilon}\bar{E}(\bar{\varepsilon}\bar{E} - 0.5)\sqrt{\pi a})$ Computed from			
	J_1^*	u_1 Regression	u_2 Regression	Lu [24]
0.0	2.112	2.097	2.105	N.A.
2.0	2.295	2.181	2.274	N.A.
4.0	2.571	2.472	2.546	N.A.
6.0	2.733	2.593	2.698	N.A.
20.0	3.228	2.819	3.117	∞ ($\beta a = \infty$)

employed to evaluate the J_1^* integral. The following data was used for the analysis of this composite configuration: $a/2h_1 = 0.67, h_1/h_2 = 1.5, L/2(h_1 + h_2) = 1.0, \bar{\varepsilon} = 1.0, \nu = 0.3$, plane strain, 2×2 Gauss quadrature. Results are presented for the normalized stress intensity factor in Table 5. These results were computed using the J_1^* integral and also by examining the near tip displacements. The agreement between the path independent integral technique and the displacement regression method is seen to be very good.

The results contained in Table 5 are very interesting from the point of view of current understandings of interface crack face problems. The analytical results of Lu [24] predict that the stress intensity factor will be unbounded if the crack tip lies at a definite material interface of the type described here. The present results indicate that the stress intensity factor remains bounded and only gradually increases as the nonhomogeneity parameter βa increases. This behavior warrants further investigation, since it appears that an extremely dramatic gradient in the slope of the elastic moduli variation is required to produce unbounded stress intensity factors.

Acknowledgements

Financial support for this work was provided by the Shell Research Foundation while the author was a student at Stanford University. Computational resources and report preparation costs were made possible by DOE Grant 12040 to Stanford University.

Appendix

The differential operators referred to in Section 2 are shown here explicitly.

$$L^1_{\lambda+n} = \frac{d^4}{d\theta^4} + [(\lambda + n)^2 + (\lambda + n - 2)^2]\frac{d^2}{d\theta^2} + [(\lambda + n)^2(\lambda + n - 2)^2] \tag{1}$$

$$L^2_{\lambda+n} = -\nu\frac{d^2}{d\theta^2} + (\lambda + n)[\lambda + n - 1 - \nu] \tag{2}$$

$$L^3_{\lambda+n} = \frac{d^2}{d\theta^2} + (\lambda + n)[1 - \nu(\lambda + n - 1)] \tag{3}$$

$$L^4_{\lambda+n} = [1 + 2\nu(\lambda + n - 1)]\frac{d^2}{d\theta^2} + (\lambda + n)[(\lambda + n - 1)((2 + \nu) - 2(\lambda + n)) + 1] \tag{4}$$

$$L^5_{\lambda+n} = -2\frac{d^3}{d\theta^3} + 2(\lambda + n)[\nu(\lambda + n - 1) - 1]\frac{d}{d\theta} \tag{5}$$

$$L^6_{\lambda+n} = 2(\lambda + n - 1)\frac{d}{d\theta} \tag{6}$$

$$L^7_{\lambda+n} = 2(1 - \lambda - n)\frac{d^2}{d\theta^2} \tag{7}$$

$$L^8_{\lambda+n} = 2[(\lambda + n)(2 - \lambda - n) - 1]\frac{d}{d\theta} \tag{8}$$

References

1. M.K. Kassir, *Journal of the Engineering Mechanics Division* 98 (1972) 457–470.
2. F. Delale and F. Erdogan, *Journal of Applied Mechanics* 50 (1983) 609–614.
3. F. Erdogan, *Journal of Applied Mechanics* 50 (1983) 992–1002.
4. C. Rogers and D.L. Clements, *Quarterly of Applied Mathematics* (1978) 315–321.
5. A. Gerasoulis and R.P. Srivastav, *International Journal of Engineering Science* 18 (1980) 239–247.
6. V.I. Fabrikant, *Engineering Fracture Mechanics* 22 (1985) 855–858.
7. R.S. Dhaliwal and B.M. Singh, *Journal of Elasticity* 8 (1978) 211–219.
8. F. Delale, *Engineering Fracture Mechanics* 22 (1985) 213–226.
9. F. Erdogan, *Journal of Applied Mechanics* 52 (1985) 823–828.
10. C. Atkinson, L.S. Xanthis and M.J.M. Bernal, *Computer Methods in Applied Mechanics and Engineering* 29 (1981) 35–49.
11. J.R. Rice, *Journal of Applied Mechanics* 35 (1968) 379–386.
12. M.L. Williams, *Journal of Applied Mechanics* 24 (1957) 109–114.
13. W.E. Boyce and R.C. DiPrima, in *Introduction of Differential Equations*, John Wiley (1970) 201–203.
14. J. Eftis, N. Subramonian, and H. Liebowitz, *Engineering Fracture Mechanics* 9 (1977) 189–210.
15. J.K. Knowles and E. Sternberg, *Archives for Rational Mechanics Analysis* 44 (1972) 187–211.
16. J.D. Eshelby, *Journal of Elasticity* 5 (1975) 321–335.
17. L.B. Freund, *Journal of Elasticity* 2 (1972) 341–349.
18. A. Ehrlacher, *Advances in Fracture Research – Fracture 81* 5 (1981) 2187–2194.
19. A.G. Herrmann and G. Herrmann, *Journal of Applied Mechanics* 48 (1981) 525–528.
20. D. Broek, *Elementary Engineering Fracture Mechanics*, Sijthoff and Noordhoff (1978).
21. T. Nishioka and S.N. Atluri, *Engineering Fracture Mechanics* 20 (1984) 193–2–8.
22. J.W. Eischen, *Engineering Fracture Mechanics* (1987) to appear.
23. O.L. Bowie, in *Mechanics of Fracture I (Methods of Analysis and Solution of Crack Problems)* Noordhoff (1973) 1–55.
24. M. Lu and F. Erdogan, *Engineering Fracture Mechanics* 18 (1983) 507–528.

Résumé. Les matériaux non homogène pris en considération dans ce travail entrent dans une classe dont les modules d'élasticité sont des fonctions continues, et généralement différentielles, des coordonnées spaciales. On deduit les champs de contraintes élastiques et de déplacements au voisinage de l'extrémité d'une fissure dans un corps non homogène à deux dimensions et fissuré, en recourant à une extension de la technique d'expansion d'une eigen-fonction due à Williams. On constate que la nature de la singularité de contrainte et de déformation est précisément de la même forme que la singularité bien connue, en forme de l'inverse de la racine carrée de la contrainte, au voisinage de l'extrémité d'une fissure dans un matériau homogène, indépendamment de la forme analytique de variation du module d'élasticité. On établit une intégrale quasi indépendante du parcours, qui se révèle utile pour calculer la vitesse de dissipation de l'énergie et les facteurs d'intensité de contrainte correspondant à des modes mixtes, dans des corps non homogènes fissurés. L'intégrale est utilisée en association avec une analyse par éléments finis, en vue de calculer les facteurs d'intensité de contraintes. Les résultats numériques sont comparés à certaines solutions exactes disponibles pour des corps non homogènes fissurés. Les corps fissurés en matériaux composites ont été traditionnellement modélisés et analysés comme s'il présentaient des modules d'élasticité discontinus. Ils sont traités ici comme des corps présentant des variations rapides mais continues des propriétés de matériaux qui les constituent.